

---

# TorchIO: a Python library for efficient loading, preprocessing, augmentation and patch-based sampling of medical images in deep learning

---

**Fernando Pérez-García**  
University College London &  
King's College London  
fernando.perezgarcia.17@ucl.ac.uk

**Rachel Sparks**  
King's College London  
rachel.sparks@kcl.ac.uk

**Sebastien Ourselin**  
King's College London  
sebastien.ourselin@kcl.ac.uk

## Abstract

We present TorchIO, an open-source Python library for efficient loading, preprocessing, augmentation and patch-based sampling of medical images for deep learning. It follows the design of PyTorch and relies on standard medical image processing libraries such as SimpleITK or NiBabel to efficiently process large 3D images during the training of convolutional neural networks. We provide multiple generic as well as magnetic-resonance-imaging-specific operations for preprocessing and augmentation of medical images. TorchIO is an open-source project with code, comprehensive examples and extensive documentation shared at <https://github.com/fepegar/torchio>.

## 1 Introduction

Due to increases in computational power of central processing units (CPUs) and graphics processing units (GPUs), greater availability of large datasets, and recent developments in learning algorithms, deep learning has become a ubiquitous research tool for solving problems related to image understanding and analysis. Convolutional neural networks (CNNs) have become the state of the art for different medical image tasks including segmentation [Çiçek et al., 2016], classification [Lu et al., 2018], reconstruction [Chen et al., 2018] and registration [Shan et al., 2018].

Compared to 2D RGB images typically used in computer vision, processing of medical images such as magnetic resonance imaging (MRI), ultrasound (US) or computerized tomography (CT) presents unique challenges. These include lack of large datasets with manual annotations, often higher computational costs due to the volumetric nature of the data, and the importance of metadata related to the physical size and position of the image.

Some groups have developed and open-sourced frameworks built on top of TensorFlow [Abadi et al., 2016] for training of CNNs with medical images [Pawlowski et al., 2017, Gibson et al., 2018]. As the popularity of PyTorch [Paszke et al., 2019] increases among researchers due to its improved usability compared to TensorFlow [He, 2019], tools compatible with this framework become more and more necessary. To reduce duplication of effort among research groups, improve experimental reproducibility and encourage open science practice, we have developed TorchIO: an open-source Python library for efficient loading, preprocessing, augmentation and patch-based sampling of medical images in deep learning.

## 2 Motivation

### 2.1 Challenges

In practice, multiple challenges need to be addressed when developing and applying deep learning algorithms to medical images.

#### 2.1.1 Metadata

In computer vision, picture elements, or *pixels*, which are assumed to be square, have a spatial relationship that comprises both proximity and depth according to the arrangement of objects in the scene and camera placement. In comparison, many medical images are reconstructed such that voxel location encodes a meaningful 3D spatial relationship. In simple terms, in 2D photo images, pixel correspondence is not necessarily related to spatial correspondence, while in medical imaging this correspondence can be assumed.

In 3D medical images, volume elements, or *voxels*, are cuboids whose size is defined by the distance between their centroids, i.e. their *spacing*. Medical images have an *offset*, which is the position in mm of the first voxel in the file with respect to some origin in the physical space. For example, in MRI, the origin is usually set at the magnet isocenter. Lastly, medical images have an *orientation* in the physical world. These three attributes are encoded in a 9-DOF,  $4 \times 4$  affine matrix. A medical image can then be defined by a 3D tensor containing voxel data and a 2D matrix representing the spatial information. These images are often stored in the Data Imaging and Communications in Medicine (DICOM) or Neuroimaging Informatics Technology Initiative (NIfTI) formats, and commonly read and processed by medical imaging frameworks such as SimpleITK [Lowe et al., 2013] or NiBabel [Brett et al., 2020].

#### 2.1.2 Limited training data

Deep learning methods typically require large amounts of annotated data, which are often scarce in clinical scenarios due to concerns over patient privacy, the financial and time burden collecting data as part of a clinical trial, and the need for annotations from highly-trained raters. Data augmentation techniques can be used to artificially increase the size of the training dataset by applying different transforms to each training instance while preserving relationship with annotations.

Traditional data augmentation operations applied in computer vision include geometrical transforms such as random rotation or zoom, colorspace transforms such as random channel swapping or kernel filters such as random Gaussian blur. Data augmentation is usually performed on the fly, i.e. every time an image is loaded from disk during training. Multiple libraries with support for computer vision data augmentation have appeared in the last years, such as Albumentations [Buslaev et al., 2020], Augmentor [Bloice et al., 2019], Kornia [Riba et al., 2019], or imgaug [Jung et al., 2020]. PyTorch also includes some computer vision transforms, mostly implemented as Pillow wrappers [wiredfool et al., 2016]. None of these libraries support reading or transformations of 3D images. Furthermore, medical images are almost always grayscale, therefore colorspace transforms are not applicable. Another example is cropping and scaling, which are common in computer vision but, if applied without care in medical images, may destroy important spatial relationships.

Some image variation is specific to medical images or even dependent on specific medical image modalities. For example, ghosting artifacts will be present in MRI if the patient moves during acquisition, and metallic implants often produce streak artifacts in CT. Simulation of these artifacts can be useful when performing augmentation of medical image data.

#### 2.1.3 Computational costs

The number of pixels in 2D images used in deep learning is rarely larger than one million. In contrast, 3D medical images often contain tens of millions of voxels. In computer vision applications, images used to train the network are grouped in batches whose size is often in the order of hundreds [Krizhevsky et al., 2012] or even thousands [Chen et al., 2020] of training instances, depending on the available GPU memory. In medical image applications, batches rarely contain more than one [Çiçek et al., 2016] or two [Milletari et al., 2016] samples due to their larger size compared to natural images. This reduces the utility of techniques such as batch normalization, which rely on

large enough batches to appropriately model dataset variance [Ioffe and Szegedy, 2015]. Moreover, larger images sizes and small batches both result in training times which are longer, hindering the experimental cycle that researchers need to experiment and tune the training hyperparameters. In cases where GPU memory is limited and the architecture is large, it is possible that not even a single volume can be processed during a single training iteration. To overcome this challenge, it is common to train using image patches randomly extracted from the volumes.

Some groups extract 2D slices from 3D volumes and perform a slice-by-slice prediction at test time [Lucena et al., 2019], aggregating the 2D inference results to generate a 3D volume. This can be seen as a specific case of patch-based training, where the size of the patches along one of the dimensions is one. Other groups extract volumetric patches for training, that are often cubes if the voxel spacing is isotropic [Kamnitsas et al., 2016, Li et al., 2017] or cuboids adapted to the anisotropic spacing of the training images [Nikolov et al., 2018].

Recent techniques such as gradient checkpointing [Chen et al., 2016], automatic mixed precision [Micikevicius et al., 2018] or reversible layers [Brügger et al., 2019] can reduce the memory burden when training with large 3D images.

### 2.1.4 Transfer learning and preprocessing

The literature has demonstrated mixed results of applying transfer learning from natural to medical images can generally be used successfully [Yang et al., 2018, Cheplygina, 2019, Raghu et al., 2019].

Images used in computer vision can generally be thought of as projections of a natural scene onto a 2D plane. Pixel values are usually encoded as an RGB triplet of bytes, i.e. they are in  $\{0, 1, 2, \dots, 255\}$ . One can often pre-train a network on a large dataset of natural images such as ImageNet [Deng et al., 2009], which contains more than 14 million labeled images, and fine-tune on a custom dataset using statistics from the original training data to preprocess each training instance.

Preprocessing of medical images is often performed on an image-per-image basis, as opposed to using statistics from the whole dataset, and the fact that these images are often bimodal (i.e. a background and a foreground) needs to be taken into account. Medical image values can be encoded in different data types with different ranges, and the meaning of a specific value can vary between different scanners or sequences. Therefore, intensity normalization methods for medical images are often more complex than those used for natural images [Nyúl and Udupa, 1999].

## 2.2 Deep learning frameworks

There are currently two major generic deep learning frameworks: TensorFlow [Abadi et al., 2016] and PyTorch [Paszke et al., 2019], primarily maintained by Google and Facebook, respectively. Although TensorFlow has traditionally been the primary choice for both research and industry, PyTorch has recently seen a strong increase in popularity, especially among the research community [He, 2019].

The main reason why researchers prefer PyTorch is that it is *Pythonic*, i.e. its design, usage, and API follow the conventions of plain Python. Moreover, the application programming interface (API) for tensor operations is tightly close to the one for NumPy multidimensional arrays [van der Walt et al., 2011]. In contrast, to use TensorFlow, researchers need to become familiar with new design elements such as sessions, placeholders, feed dictionaries or static graphs. In PyTorch, objects are standard Python classes and variables, and a dynamic graph makes debugging intuitive and familiar. These differences are decreased with the recent release of TensorFlow 2, whose eager mode makes usage reminiscent of Python.

## 3 Related work

The Deep Learning Toolkit (DLTK) [Pawlowski et al., 2017] and NiftyNet [Gibson et al., 2018] are deep learning platforms designed explicitly for medical image processing and using the TensorFlow 1 platform. They provide implementations of some popular architectures such as U-Net [Çiçek et al., 2016], and can be used to train 3D CNNs for different tasks. The last set of substantial commits on the DLTK repository are from June 2018, which suggests that the code is not actively maintained. NiftyNet includes some preprocessing and augmentation operations specifically for medical images, such as histogram standardization [Nyúl et al., 2000] and random bias field augmentation [Van Leem-

put et al., 1999, Sudre et al., 2017], both implemented using NumPy. It is designed to be used through a high-level configuration file, making its usage slightly cumbersome for researchers who desire lower-level access to alter or augment its features.

The `medicaltorch` library [Perone et al., 2018] closely follows the PyTorch design, and provides some functionalities for preprocessing, augmentation and training of 3D medical images. However, it does not leverage the power of specialized medical image processing libraries such as SimpleITK [Lowekamp et al., 2013]. For example, the random 3D rotation is performed to the volume slice by slice along a specified axis using PyTorch. If rotations around more axes are desired, computation time will increase linearly with the number of rotations. Moreover, interpolation applied at multiple resampling operations degrades the image. In contrast, multiple rotations, translations, shearings, etc. may be composed into a single affine transform and applied once in 3D, reducing resampling artifacts and computational costs. As DLTK, this library has not seen much activity since 2018.

The `batchgenerators` library [Isensee et al., 2020] includes custom dataset and data loader classes for multithreaded loading of 3D medical images, that were implemented before data loaders were available in PyTorch. In the usage examples from GitHub, preprocessing is applied to the whole dataset before training. Then, spatial data augmentation is performed at volume level, from which one patch is extracted and intensity augmentation is performed at the patch level. In this approach, only one patch is extracted from each volume. Transforms in `batchgenerators` are mostly implemented using NumPy [van der Walt et al., 2011] and SciPy [Virtanen et al., 2020].

## 4 Methods

We developed TorchIO, a Python library that focuses on medical image processing for deep learning. Following the PyTorch philosophy [Paszke et al., 2019], we designed TorchIO with an emphasis on simplicity and usability.

As part of simplicity and usability, we used PyTorch classes and infrastructure where appropriate. This has the added advantage of a fast learning curve for users and, we hope, reduced barrier to adapt the framework to new use cases.

Volumes can be loaded and processed in parallel using `torch.utils.data.DataLoader`, and image datasets inherit from `torch.utils.data.Dataset` (`torch` is the name of the PyTorch Python package). Patch samplers, which yield image patches, inherit from `torch.utils.data.IterableDataset`. The transforms API is very similar to `torchvision.transforms` module. For example, TorchIO transforms are composed using `torchvision.transforms.Compose`. Stochasticity in random transforms is always determined by PyTorch functions to ensure multiprocessing consistence.

TorchIO uses computer vision augmentations such as random affine transformation or random blur where appropriate, but we implemented them using medical imaging libraries [Lowekamp et al., 2013, Brett et al., 2020] that take into account the specific nature of medical images (see Section 2.1.1).

Preprocessing and sampling features are similar to the ones available in NiftyNet. This ensures a smooth transition from NiftyNet input/output system to the TorchIO environment.

In contrast with DLTK or NiftyNet, we do not implement architectures, loss functions or training applications, in order to limit the scope of the library for the sake of modularity.

## 5 Results

TorchIO code is available on GitHub<sup>1</sup>. Detailed API documentation is hosted on Read The Docs<sup>2</sup> and Jupyter notebook tutorials are hosted on Google Colaboratory, where users can run examples online<sup>3</sup>. The software can be installed with a single line of code on Windows, macOS or Linux using the Pip Installs Packages (PIP) package manager: `pip install torchio`.

---

<sup>1</sup><https://github.com/fepegar/torchio>

<sup>2</sup><https://torchio.readthedocs.io/>

<sup>3</sup><https://colab.research.google.com/drive/112NTL8uJXzcMw4PQbUvMQN-WH1VwQS3i>

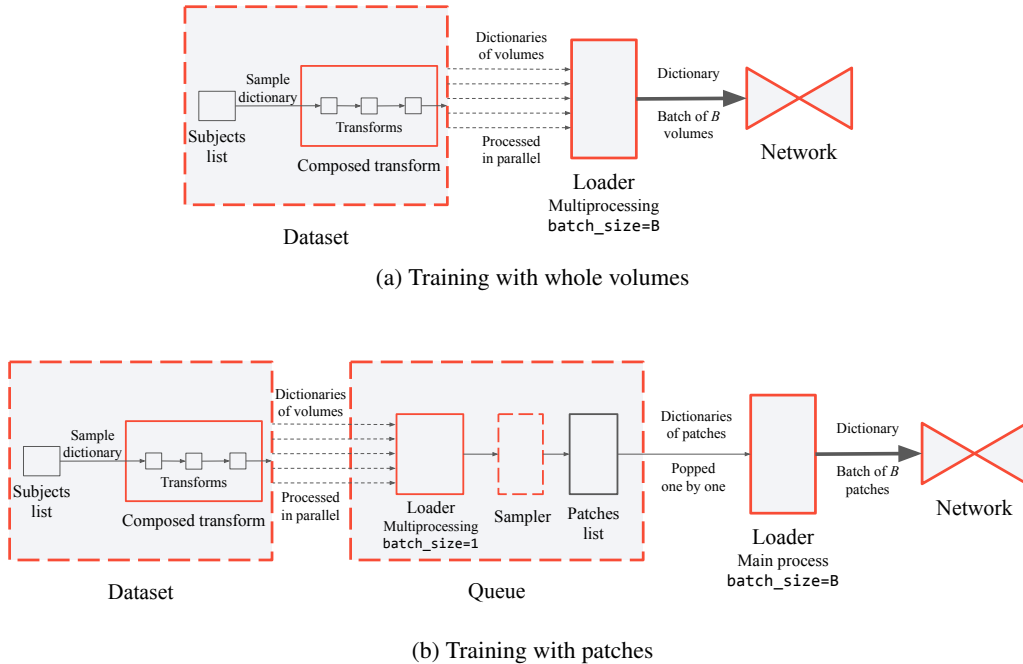


Figure 1: Diagram of data pipelines for training with whole volumes (top) and patches (bottom). Boxes with a red border are PyTorch classes (—) or inherit from PyTorch classes (- - -).

## 5.1 Loading

The `torchio.ImagesDataset` inherits from `torch.utils.data.Dataset` and can be used to load medical images in popular formats such as NIfTI, DICOM, Medical Imaging NetCDF (MINC) or Nearly Raw Raster Data (NRRD) using medical images libraries such as NiBabel or SimpleITK. `torchio.ImagesDataset` can be used as is or customized by inheriting the class. As an example, the Information eXtraction from Images (IXI) dataset<sup>4</sup> can be downloaded using `torchio.datasets.IXI`, which is a subclass of `torchio.ImagesDataset`. `torchio.ImagesDataset` can be directly used with PyTorch data loaders to leverage their multiprocessing capabilities. If a transform or a composition of transforms is passed to this class, it will be applied to the image after loading. Figure 1 illustrates a typical TorchIO pipeline.

## 5.2 Preprocessing

Preprocessing transforms include spatial operations applied to medical images such as resampling (e.g. to make voxel spacing isotropic for all training samples) or reorientation (e.g. so that all training samples are oriented in the same way) using NiBabel. Spatial preprocessing is important as CNNs do not generally take into account meta-information related to medical images (see Section 2.1.1).

TorchIO provides intensity normalization techniques including min-max scaling or standardization, which are computed using pure PyTorch. In this context, standardization refers to correcting voxel intensity values to have zero mean and unit variance. A binary image, such as a mask representing the foreground or structures of interest, can be used to define the set of voxels to be taken into account when computing statistics for intensity normalization.

We also provide a method for MRI histogram standardization [Nyúl et al., 2000, Gibson et al., 2018], computed using NumPy, which may be used to overcome the differences in intensity distributions between images acquired using different scanners or sequences.

<sup>4</sup><https://brain-development.org/ixi-dataset/>

### 5.3 Augmentation

TorchIO includes spatial transforms such as random flipping using PyTorch and random affine and elastic deformation transforms using SimpleITK.

Intensity augmentation transforms include random Gaussian blur using a SimpleITK filter and addition of random Gaussian noise using pure PyTorch.

TorchIO provides several MRI-specific augmentation transforms related to k-space, which are described below. An MR image is usually reconstructed as the magnitude of the inverse Fourier transform of the k-space signal, which is populated with the signals generated by the sample after a radio-frequency pulse. These signals are modulated using coils that create magnetic gradients in the scanner.

Artifacts are created by using k-space transforms to perturb the Fourier space and generate corresponding intensity artifacts in image space. The forward and inverse Fourier transforms are computed using the Fast Fourier Transform (FFT) algorithm [Cooley and Tukey, 1965] implemented in NumPy. Figure 2 shows examples of augmentation transforms implemented in TorchIO.

**Random k-space spike artifact** Gradients applied at a very high duty cycle may produce bad data points, or spikes of noise, in k-space [Zhuo and Gullapalli, 2006]. These points in k-space generate a spike artifact, also known as Herringbone, crisscross or corduroy artifact, which manifests as uniformly-separated stripes in image space, as shown in Fig. 2i. This type of data augmentation has recently been used to estimate uncertainty through a heteroscedastic noise model [Shaw et al., 2020].

**Random k-space motion artifact** The k-space is often populated line by line, and the sample in the scanner is assumed to remain static. If a patient moves during the MRI acquisition, motion artifacts will appear in the reconstructed image. We implemented a method to simulate random motion artifacts (see Fig. 2h) that has been used for data augmentation to model uncertainty and improve segmentation [Shaw et al., 2019].

**Random k-space ghosting artifact** Organs motion such as respiration or cardiac pulsation may generate ghosting artifacts along the phase-encoding direction [Zhuo and Gullapalli, 2006] (see Fig. 2j).

**Random bias field artifact** Inhomogeneity of the static magnetic field in the MRI scanner produces intensity artifacts of very low spatial frequency along the entirety of the image. These artifacts can be simulated using polynomial basis functions [Van Leemput et al., 1999, Sudre et al., 2017, Gibson et al., 2018], as shown in Fig. 2g.

Although current domain-specific data augmentation transforms available in TorchIO are mostly related to MRI, we encourage users to contribute physics-based data augmentation techniques for US or CT [Omigbodun et al., 2019].

### 5.4 Patch-based sampling

Memory limitations often require training and inference steps to be performed using image patches, instead of the whole volumes, as explained in Section 2.1.3. A training iteration performed on a GPU is usually faster than loading, preprocessing, augmenting and cropping a volume on a CPU. Therefore, it is beneficial to prepare (i.e. load, preprocess and augment) the volumes using multiprocessing CPU techniques and then sample multiple patches from each volume. The sampled patches are added to a buffer or *queue* until the next training iteration, at which point they are loaded onto the GPU. Parallel processing can be performed by passing a `torchio.ImagesDataset` to a PyTorch data loader (`torch.utils.data.DataLoader`), as explained in Section 5.1.

Following the NiftyNet design, we implemented a queueing system where samplers behave as generators that yield patches from random locations in volumes contained in the subjects dataset. At the beginning of the training pipeline, the subjects dataset may be shuffled. A loader queries the dataset, which then loads and processes volumes in parallel. A sampler fills the queue with patches extracted from the volumes, and the queue may be shuffled if specified. In the background, the data

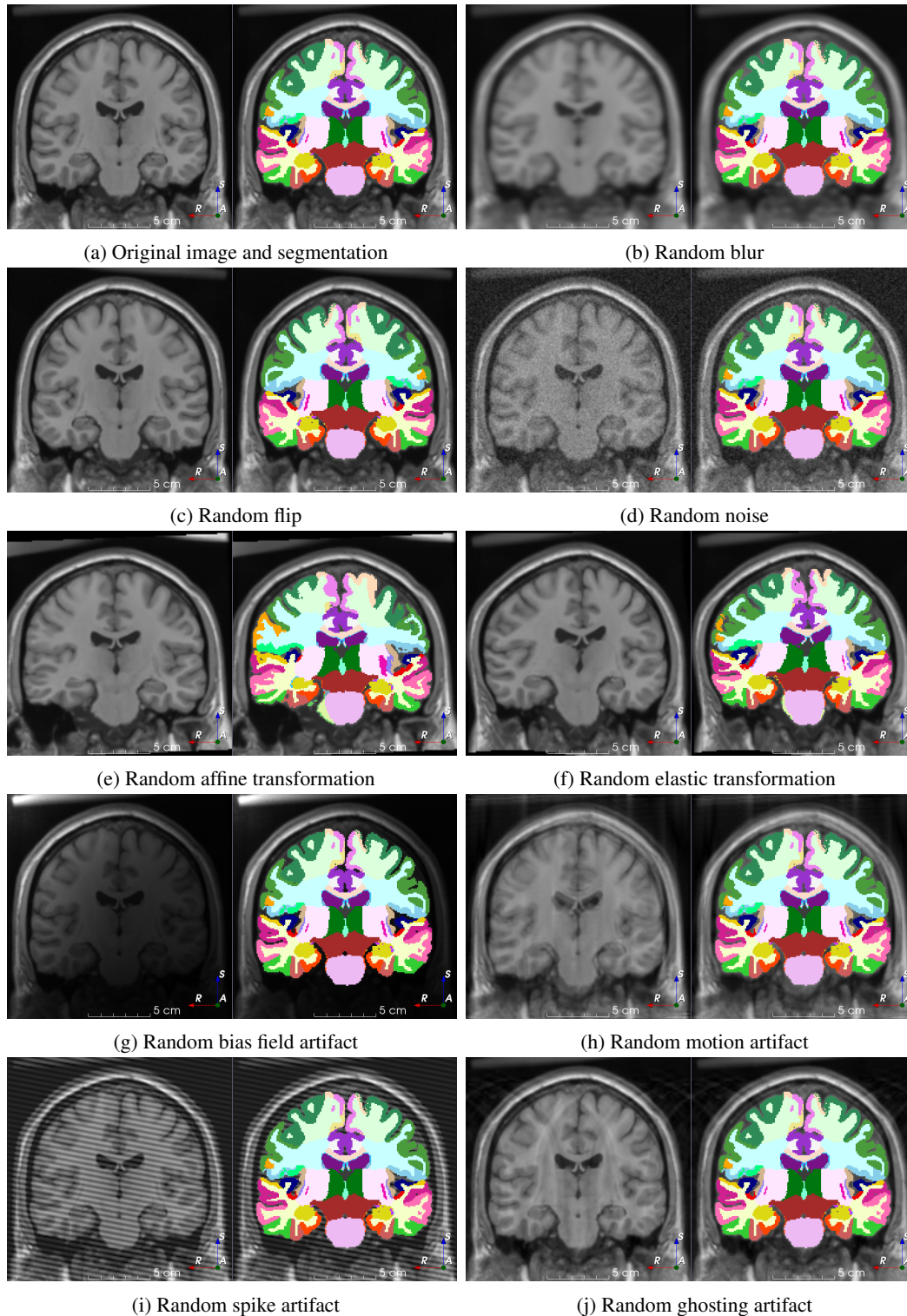


Figure 2: A selection of data augmentation techniques currently available in TorchIO. Each example is presented as a pair of images composed of the transformed image and a corresponding transformed annotation. Note that all images are a 2D coronal slice of the transformed 3D volumes. The MRI corresponds to the Montreal Neurological Institute (MNI) Colin 27 average brain [Holmes et al., 1998]. Annotations were generated using an automated brain parcellation algorithm [Cardoso et al., 2015].

loader continues querying the dataset. The queue is then refilled with new patches when empty. When patches from all subjects have been extracted, the subjects dataset is reshuffled. See diagram Fig. 1b for a visual representation of the patch-based training in TorchIO.

We implemented an aggregator for patch-wise inference of large volumes, following a similar design in NiftyNet. The aggregator receives —potentially overlapping— patches that have been sampled by a grid sampler and passed into a trained network, and aggregates them into an output array with the same size as the original volume from which the patches are generated.

## 5.5 Command-line interface

The provided command-line interface (CLI) tool `torchio-transform` allows the user to experiment by applying a transform to an image file without using Python. The tool can also be used in shell scripts to preprocess and augment datasets in cases where large storage is available and on-the-fly loading needs to be faster.

## 6 Examples

We provide in the documentation a comprehensive example of training a custom implementation of 3D U-Net [Pérez-García, 2020] to perform brain segmentation from MRI using TorchIO for image processing.

To create the dataset, we 1) segmented the brain in 566  $T_1$ -weighted MR images from the IXI dataset using geodesical information flows (GIF) [Cardoso et al., 2015], 2) registered the images to an Montreal Neurological Institute (MNI) template using NiftyReg [Modat et al., 2014], and 3) resampled the images to have a size of  $I \times J \times K = 83 \times 44 \times 55$  after a Gaussian filter (SimpleITK) to reduce aliasing. We resized the images so that the example can be run in a short time, with little resources.

For each subject  $m$ , an instance of `torchio.Subject` is created with the corresponding images. Images  $(X_m^{C_x \times I \times J \times K}, Y_m^{C_y \times I \times J \times K})$  corresponding to each subject are two specific instances of `torchio.Image`: an intensity image (`torchio.INTENSITY`) representing the MRI and a binary image (`torchio.LABEL`) representing the brain segmentation, where  $C_x = 1$  (single input channel) and  $C_y = 2$  (background and foreground). A Python list of subjects is created.

The preprocessing and augmentation pipelines are defined as Python lists containing instances of `torchio.transforms.Transform`. In this example, the operations for the training set are `Rescale`, `RandomMotion`, `HistogramStandardization`, `RandomBiasField`, `ZNormalization`, `RandomNoise`, `ToCanonical`, `Resample`, `CenterCropOrPad`, `RandomFlip`, `RandomAffine` and `RandomElasticDeformation`, all imported from `torchio.transforms`. For the validation set, the following subset of preprocessing transforms are used: `HistogramStandardization`, `ZNormalization`, `ToCanonical`, `Resample` and `CenterCropOrPad`. TorchIO determines the appropriate image types to apply each transform to, with intensity transforms applied to images with type `torchio.INTENSITY` and spatial transforms applied to all images.

Intensity transforms are applied by default only to the MRI, whereas spatial transforms are applied to both the MRI and the segmentation. Each list is composed into a single transform with PyTorch using `torchvision.transforms.Compose`.

The list of subjects is split into a training list and a validation list and two instances of `torchio.ImagesDataset` are created, using their corresponding composed transforms.

The following pipeline descriptions apply to both training and validation.

### 6.1 Case 1: training with whole volumes

The rest of the pipeline is simple when using whole volumes for training, as shown in Fig. 1a. First, we instantiate a `torch.utils.data.DataLoader` from the training dataset, specifying the batch size  $B$  and the number of CPU cores that will be used to prepare the volumes.

Then, the training loop starts. The loader starts spawning processes that query the dataset for samples, where a sample is a dictionary containing the images corresponding to a subject.

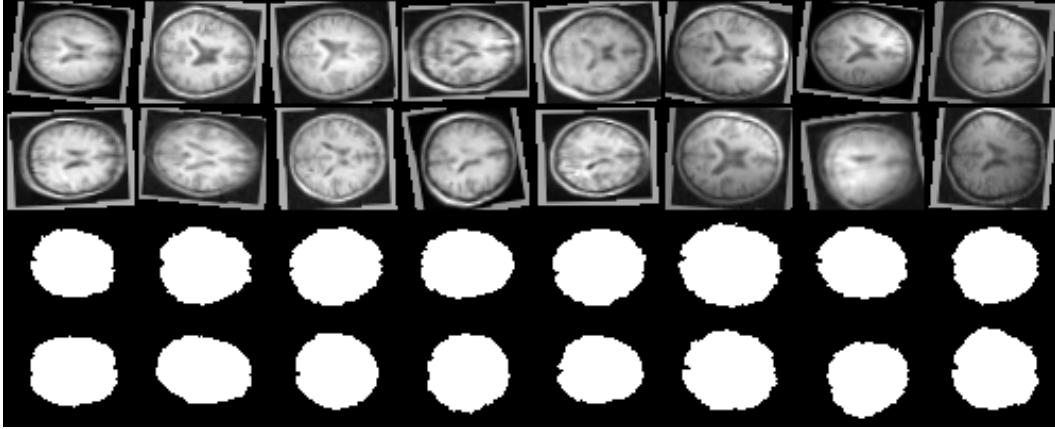


Figure 3: Example of a training batch of size  $B = 16$  when training with whole volumes. Top: input MR images after preprocessing and augmentation; bottom: corresponding labels. Note that these images are 3D, but only one axial slice of each image is shown here for visualization purposes.

The dataset loads and applies the transform to the images of the subject. Transforms such as `CenterCropOrPad` and `Resample` may modify the number of voxels to  $I' \times J' \times K'$ . At each iteration, the loader composes a batch  $n$  with  $B = 16$  volumes into a Python dictionary. The tensors  $(X_n^{B \times C_x \times I' \times J' \times K'}, Y_n^{B \times C_y \times I' \times J' \times K'})$  corresponding to voxel intensity values are extracted from the batch dictionary, and the training iteration is performed. Figure 3 shows an example of a batch of volumes.

Inference is trivial as batches can be generated by a data loader in the same manner.

Note that training with whole volumes is rare unless large GPUs are available.

## 6.2 Case 2: training with patches

To train with patches, the `torchio.ImagesDataset` is passed to a `torchio.Queue`, which also inherits from `torch.utils.data.Dataset` (see Section 5.4). The `torch.utils.data.DataLoader`  $L_x(b)$  is connected to the queue to generate batches of size  $b = 32$ . This loader does not use multiprocessing, patches are just popped from the queue.

The queue internally uses the `torch.utils.data.DataLoader`  $L_X(1)$  that is connected to the `torchio.ImagesDataset` to load volumes with multiprocessing. Each volume is passed to the `torchio.data.ImageSampler`, which inherits from `torch.utils.data.IterableDataset`. The sampler extracts  $s$  patches of size  $i \times j \times k$  from each volume and the patches are added to the queue until it contains  $q$  patches. In the example,  $s = 5$ ,  $q = 300$  and  $i = j = k = 24$ .

At each iteration,  $L_x$  composes a batch  $n$  with  $b$  patches into a Python dictionary. The tensors  $(x_n^{b \times C_x \times i \times j \times k}, y_n^{b \times C_y \times i \times j \times k})$  are extracted from the batch dictionary and the training iteration is executed. Figures 1b and 4 show a diagram of the training pipeline and an example of a batch of patches, respectively.

To perform a dense prediction across a volume, the volume is loaded by the dataset instance and passed to a `torchio.inference.GridSampler`. The sampler creates a uniform grid of patches that can overlap to reduce the border artifacts introduced by padded convolutions. The sampler is passed to a `torchio.utils.data.DataLoader` that extracts batches of patches that are passed through the network for inference. The predicted batches and their original locations in the volume are passed to a `torchio.inference.GridAggregator` which builds the output volume from the batches data and location.

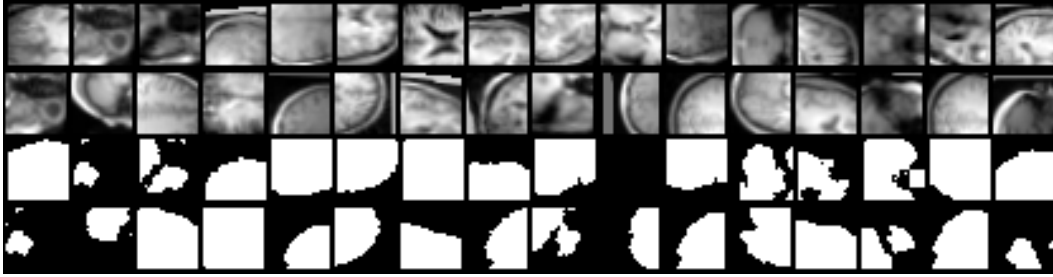


Figure 4: Example of a training batch of size  $B = 32$  when training with image patches. Top: input patches of MR images after preprocessing and augmentation; bottom: corresponding labels. Note that these are 3D patches, but only one axial slice is shown here for visualization purposes.

## 7 Conclusion

We present TorchIO, a new library to efficiently handle medical imaging data during training of CNNs. It is designed in the style of the deep learning framework PyTorch, and provides medical imaging specific features such as image reorientation and simulation of MRI artifacts for data augmentation.

In the future, we will work on extending the preprocessing and augmentation transforms to different medical imaging modalities such as CT or US. The source code, as well as examples and documentation, are made publicly available online on GitHub. We welcome feedback, feature requests and contributions to the library, either by creating issues on the GitHub repository or by emailing the authors.

## Acknowledgments

We thank the NiftyNet team for their support. We also would like to thank Reuben Dorent and Romain Valabregue for their valuable insight.

This work is supported by the EPSRC-funded UCL Centre for Doctoral Training in Medical Imaging (EP/L016478/1). This publication represents in part independent research commissioned by the Wellcome Trust Health Innovation Challenge Fund (WT106882). The views expressed in this publication are those of the authors and not necessarily those of the Wellcome Trust.

## References

- M. Abadi, A. Agarwal, P. Barham, E. Brevdo, Z. Chen, C. Citro, G. S. Corrado, A. Davis, J. Dean, M. Devin, S. Ghemawat, I. Goodfellow, A. Harp, G. Irving, M. Isard, Y. Jia, R. Jozefowicz, L. Kaiser, M. Kudlur, J. Levenberg, D. Mane, R. Monga, S. Moore, D. Murray, C. Olah, M. Schuster, J. Shlens, B. Steiner, I. Sutskever, K. Talwar, P. Tucker, V. Vanhoucke, V. Vasudevan, F. Viegas, O. Vinyals, P. Warden, M. Wattenberg, M. Wicke, Y. Yu, and X. Zheng. TensorFlow: Large-Scale Machine Learning on Heterogeneous Distributed Systems. *arXiv:1603.04467 [cs]*, Mar. 2016. URL <http://arxiv.org/abs/1603.04467>. arXiv: 1603.04467.
- M. D. Bloice, P. M. Roth, and A. Holzinger. Biomedical image augmentation using Augmentor. *Bioinformatics*, 35(21):4522–4524, Nov. 2019. ISSN 1367-4803. doi: 10.1093/bioinformatics/btz259. URL <https://academic.oup.com/bioinformatics/article/35/21/4522/5466454>.
- M. Brett, C. J. Markiewicz, M. Hanke, M.-A. Côté, B. Cipollini, P. McCarthy, C. P. Cheng, Y. O. Halchenko, M. Cottaar, S. Ghosh, E. Larson, D. Wassermann, S. Gerhard, G. R. Lee, H.-T. Wang, E. Kastman, A. Rokem, C. Madison, F. C. Morency, B. Moloney, M. Goncalves, C. Riddell, C. Burns, J. Millman, A. Gramfort, J. Leppäkangas, R. Markello, J. J. van den Bosch, R. D. Vincent, H. Braun, K. Subramaniam, D. Jarecka, K. J. Gorgolewski, P. R. Raamana, B. N. Nichols, E. M. Baker, S. Hayashi, B. Pinsard, C. Haselgrove, M. Hymers, O. Esteban, S. Koudoro, N. N. Oosterhof, B. Amirbekian, I. Nimmo-Smith, L. Nguyen, S. Reddigari, S. St-Jean, E. Panfilov, E. Garyfallidis, G. Varoquaux, J. Kaczmarzyk, J. H. Legarreta, K. S. Hahn, O. P. Hinds, B. Fauber, J.-B. Poline, J. Stutters, K. Jordan, M. Cieslak, M. E. Moreno, V. Haenel, Y. Schwartz, B. C. Darwin,

- B. Thirion, D. Papadopoulos Orfanos, F. Pérez-García, I. Solovey, I. Gonzalez, J. Palasubramaniam, J. Lecher, K. Leinweber, K. Raktivan, P. Fischer, P. Gervais, S. Gadde, T. Ballinger, T. Roos, V. R. Reddam, and freec84. nipy/nibabel: 3.0.1, Jan. 2020. URL <https://zenodo.org/record/3628482#.XlyGkJP7S8o>.
- R. Brügger, C. F. Baumgartner, and E. Konukoglu. A Partially Reversible U-Net for Memory-Efficient Volumetric Image Segmentation. *arXiv:1906.06148 [cs, eess]*, June 2019. URL <http://arxiv.org/abs/1906.06148>. arXiv: 1906.06148.
- A. Buslaev, A. Parinov, E. Khvedchenya, V. I. Iglovikov, and A. A. Kalinin. Alumentations: fast and flexible image augmentations. *Information*, 11(2):125, Feb. 2020. ISSN 2078-2489. doi: 10.3390/info11020125. URL <http://arxiv.org/abs/1809.06839>. arXiv: 1809.06839.
- M. J. Cardoso, M. Modat, R. Wolz, A. Melbourne, D. Cash, D. Rueckert, and S. Ourselin. Geodesic Information Flows: Spatially-Variant Graphs and Their Application to Segmentation and Fusion. *IEEE Transactions on Medical Imaging*, 34(9):1976–1988, Sept. 2015. ISSN 0278-0062. doi: 10.1109/TMI.2015.2418298.
- F. Chen, V. Taviani, I. Malkiel, J. Y. Cheng, J. I. Tamir, J. Shaikh, S. T. Chang, C. J. Hardy, J. M. Pauly, and S. S. Vasanaawala. Variable-Density Single-Shot Fast Spin-Echo MRI with Deep Learning Reconstruction by Using Variational Networks. *Radiology*, 289(2):366–373, July 2018. ISSN 0033-8419. doi: 10.1148/radiol.2018180445. URL <https://pubs.rsna.org/doi/10.1148/radiol.2018180445>.
- T. Chen, B. Xu, C. Zhang, and C. Guestrin. Training Deep Nets with Sublinear Memory Cost. *arXiv:1604.06174 [cs]*, Apr. 2016. URL <http://arxiv.org/abs/1604.06174>. arXiv: 1604.06174.
- T. Chen, S. Kornblith, M. Norouzi, and G. Hinton. A Simple Framework for Contrastive Learning of Visual Representations. *arXiv:2002.05709 [cs, stat]*, Feb. 2020. URL <http://arxiv.org/abs/2002.05709>. arXiv: 2002.05709.
- V. Cheplygina. Cats or CAT scans: transfer learning from natural or medical image source datasets? *Current Opinion in Biomedical Engineering*, 9:21–27, Mar. 2019. ISSN 24684511. doi: 10.1016/j.cobme.2018.12.005. URL <http://arxiv.org/abs/1810.05444>. arXiv: 1810.05444.
- Ö. Çiçek, A. Abdulkadir, S. S. Lienkamp, T. Brox, and O. Ronneberger. 3D U-Net: Learning Dense Volumetric Segmentation from Sparse Annotation. *arXiv:1606.06650 [cs]*, June 2016. URL <http://arxiv.org/abs/1606.06650>.
- J. W. Cooley and J. W. Tukey. An Algorithm for the Machine Calculation of Complex Fourier Series. *Mathematics of Computation*, 19(90):297–301, 1965. ISSN 0025-5718. doi: 10.2307/2003354. URL <https://www.jstor.org/stable/2003354>.
- J. Deng, W. Dong, R. Socher, L.-J. Li, K. Li, and L. Fei-Fei. ImageNet: A large-scale hierarchical image database. In *2009 IEEE Conference on Computer Vision and Pattern Recognition*, pages 248–255, June 2009. doi: 10.1109/CVPR.2009.5206848. ISSN: 1063-6919.
- E. Gibson, W. Li, C. Sudre, L. Fidon, D. I. Shkir, G. Wang, Z. Eaton-Rosen, R. Gray, T. Doel, Y. Hu, T. Whyntie, P. Nachev, M. Modat, D. C. Barratt, S. Ourselin, M. J. Cardoso, and T. Vercauteren. NiftyNet: a deep-learning platform for medical imaging. *Computer Methods and Programs in Biomedicine*, 158:113–122, May 2018. ISSN 0169-2607. doi: 10.1016/j.cmpb.2018.01.025. URL <http://www.sciencedirect.com/science/article/pii/S0169260717311823>.
- H. He. The State of Machine Learning Frameworks in 2019, Oct. 2019. URL <http://bit.ly/3cjpliJ>.
- C. J. Holmes, R. Hoge, L. Collins, R. Woods, A. W. Toga, and A. C. Evans. Enhancement of MR images using registration for signal averaging. *Journal of Computer Assisted Tomography*, 22(2): 324–333, Apr. 1998. ISSN 0363-8715. doi: 10.1097/00004728-199803000-00032.
- S. Ioffe and C. Szegedy. Batch Normalization: Accelerating Deep Network Training by Reducing Internal Covariate Shift. *arXiv:1502.03167 [cs]*, Mar. 2015. URL <http://arxiv.org/abs/1502.03167>. arXiv: 1502.03167.

- F. Isensee, P. Jäger, J. Wasserthal, D. Zimmerer, J. Petersen, S. Kohl, J. Schock, A. Klein, T. Roß, S. Wirkert, P. Neher, S. Dinkelacker, G. Köhler, and K. Maier-Hein. batchgenerators - a python framework for data augmentation, Jan. 2020. URL <https://zenodo.org/record/3632567#.Xlqnb5P7S8o>.
- A. B. Jung, K. Wada, J. Crall, S. Tanaka, J. Graving, C. Reinders, S. Yadav, J. Banerjee, G. Vecsei, A. Kraft, Z. Rui, J. Borovec, C. Vallentin, S. Zhydenko, K. Pfeiffer, B. Cook, I. Fernández, F.-M. De Rainville, C.-H. Weng, A. Ayala-Acevedo, R. Meudec, M. Laporte, and others. imgaug, 2020. URL <https://github.com/aleju/imgaug>.
- K. Kamnitsas, E. Ferrante, S. Parisot, C. Ledig, A. V. Nori, A. Criminisi, D. Rueckert, and B. Glocker. DeepMedic for Brain Tumor Segmentation. In *Brainlesion: Glioma, Multiple Sclerosis, Stroke and Traumatic Brain Injuries*, Lecture Notes in Computer Science, pages 138–149. Springer, Cham, Oct. 2016. ISBN 978-3-319-55523-2 978-3-319-55524-9. doi: 10.1007/978-3-319-55524-9\_14. URL [https://link.springer.com/chapter/10.1007/978-3-319-55524-9\\_14](https://link.springer.com/chapter/10.1007/978-3-319-55524-9_14).
- A. Krizhevsky, I. Sutskever, and G. E. Hinton. ImageNet Classification with Deep Convolutional Neural Networks. In *Proceedings of the 25th International Conference on Neural Information Processing Systems - Volume 1, NIPS’12*, pages 1097–1105, USA, 2012. Curran Associates Inc. URL <http://dl.acm.org/citation.cfm?id=2999134.2999257>.
- W. Li, G. Wang, L. Fidon, S. Ourselin, M. J. Cardoso, and T. Vercauteren. On the Compactness, Efficiency, and Representation of 3D Convolutional Networks: Brain Parcellation as a Pretext Task. *arXiv:1707.01992*, 10265:348–360, 2017. doi: 10.1007/978-3-319-59050-9\_28. URL <http://arxiv.org/abs/1707.01992>.
- B. C. Lowekamp, D. T. Chen, L. Ibáñez, and D. Blezek. The Design of SimpleITK. *Frontiers in Neuroinformatics*, 7:45, 2013. ISSN 1662-5196. doi: 10.3389/fninf.2013.00045.
- D. Lu, K. Popuri, G. W. Ding, R. Balachandar, M. F. Beg, and Alzheimer’s Disease Neuroimaging Initiative. Multimodal and Multiscale Deep Neural Networks for the Early Diagnosis of Alzheimer’s Disease using structural MR and FDG-PET images. *Scientific Reports*, 8(1):5697, 2018. ISSN 2045-2322. doi: 10.1038/s41598-018-22871-z.
- O. Lucena, R. Souza, L. Rittner, R. Frayne, and R. Lotufo. Convolutional neural networks for skull-stripping in brain MR imaging using silver standard masks. *Artificial Intelligence in Medicine*, 98: 48–58, 2019. ISSN 1873-2860. doi: 10.1016/j.artmed.2019.06.008.
- P. Micikevicius, S. Narang, J. Alben, G. Diamos, E. Elsen, D. Garcia, B. Ginsburg, M. Houston, O. Kuchaiev, G. Venkatesh, and H. Wu. Mixed Precision Training. *arXiv:1710.03740 [cs, stat]*, Feb. 2018. URL <http://arxiv.org/abs/1710.03740>. arXiv: 1710.03740.
- F. Milletari, N. Navab, and S.-A. Ahmadi. V-Net: Fully Convolutional Neural Networks for Volumetric Medical Image Segmentation. *arXiv:1606.04797 [cs]*, June 2016. URL <http://arxiv.org/abs/1606.04797>. arXiv: 1606.04797.
- M. Modat, D. M. Cash, P. Daga, G. P. Winston, J. S. Duncan, and S. Ourselin. Global image registration using a symmetric block-matching approach. *Journal of Medical Imaging*, 1(2), July 2014. ISSN 2329-4302. doi: 10.1117/1.JMI.1.2.024003. URL <https://www.ncbi.nlm.nih.gov/pmc/articles/PMC4478989/>.
- S. Nikolov, S. Blackwell, R. Mendes, J. De Fauw, C. Meyer, C. Hughes, H. Askham, B. Romera-Paredes, A. Karthikesalingam, C. Chu, D. Carnell, C. Boon, D. D’Souza, S. A. Moinuddin, K. Sullivan, D. R. Consortium, H. Montgomery, G. Rees, R. Sharma, M. Suleyman, T. Back, J. R. Ledsam, and O. Ronneberger. Deep learning to achieve clinically applicable segmentation of head and neck anatomy for radiotherapy. *arXiv:1809.04430 [physics, stat]*, Sept. 2018. URL <http://arxiv.org/abs/1809.04430>. arXiv: 1809.04430.
- L. G. Nyúl and J. K. Udupa. On standardizing the MR image intensity scale. *Magnetic Resonance in Medicine*, 42(6):1072–1081, Dec. 1999. ISSN 0740-3194. doi: 10.1002/(sici)1522-2594(199912)42:6<1072::aid-mrm11>3.0.co;2-m.

- L. G. Nyúl, J. K. Udupa, and X. Zhang. New variants of a method of MRI scale standardization. *IEEE transactions on medical imaging*, 19(2):143–150, Feb. 2000. ISSN 0278-0062. doi: 10.1109/42.836373.
- A. O. Omigbodun, F. Noo, M. McNitt-Gray, W. Hsu, and S. S. Hsieh. The effects of physics-based data augmentation on the generalizability of deep neural networks: Demonstration on nodule false-positive reduction. *Medical Physics*, 46(10):4563–4574, 2019. ISSN 2473-4209. doi: 10.1002/mp.13755. URL <https://aapm.onlinelibrary.wiley.com/doi/abs/10.1002/mp.13755>.
- A. Paszke, S. Gross, F. Massa, A. Lerer, J. Bradbury, G. Chanan, T. Killeen, Z. Lin, N. Gimelshein, L. Antiga, A. Desmaison, A. Kopf, E. Yang, Z. DeVito, M. Raison, A. Tejani, S. Chilamkurthy, B. Steiner, L. Fang, J. Bai, and S. Chintala. PyTorch: An Imperative Style, High-Performance Deep Learning Library. In H. Wallach, H. Larochelle, A. Beygelzimer, F. d. Alché-Buc, E. Fox, and R. Garnett, editors, *Advances in Neural Information Processing Systems 32*, pages 8026–8037. Curran Associates, Inc., 2019. URL <http://papers.nips.cc/paper/9015-pytorch-an-imperative-style-high-performance-deep-learning-library.pdf>.
- N. Pawlowski, S. I. Ktena, M. C. H. Lee, B. Kainz, D. Rueckert, B. Glocker, and M. Rajchl. DLTK: State of the Art Reference Implementations for Deep Learning on Medical Images. *arXiv:1711.06853 [cs]*, Nov. 2017. URL <http://arxiv.org/abs/1711.06853>. arXiv: 1711.06853.
- F. Pérez-García. fepegar/unet: PyTorch implementation of 2D and 3D U-Net, Mar. 2020. URL <https://zenodo.org/record/3697931#.XmD82XX7RhE>.
- C. S. Perone, cclauss, E. Saravia, P. L. Ballester, and MohitTare. perone/medicalltorch: Release v0.2, Nov. 2018. URL <https://zenodo.org/record/1495335#.X1qwUZP7S8o>.
- M. Raghu, C. Zhang, J. Kleinberg, and S. Bengio. Transfusion: Understanding Transfer Learning for Medical Imaging. *arXiv:1902.07208 [cs, stat]*, Oct. 2019. URL <http://arxiv.org/abs/1902.07208>. arXiv: 1902.07208.
- E. Riba, D. Mishkin, D. Ponsa, E. Rublee, and G. Bradski. Kornia: an Open Source Differentiable Computer Vision Library for PyTorch. *arXiv:1910.02190 [cs]*, Oct. 2019. URL <http://arxiv.org/abs/1910.02190>. arXiv: 1910.02190.
- S. Shan, W. Yan, X. Guo, E. I.-C. Chang, Y. Fan, and Y. Xu. Unsupervised End-to-end Learning for Deformable Medical Image Registration. *arXiv:1711.08608 [cs]*, Jan. 2018. URL <http://arxiv.org/abs/1711.08608>. arXiv: 1711.08608.
- R. Shaw, C. Sudre, S. Ourselin, and M. J. Cardoso. MRI k-Space Motion Artefact Augmentation: Model Robustness and Task-Specific Uncertainty. In *International Conference on Medical Imaging with Deep Learning*, pages 427–436, May 2019. URL <http://proceedings.mlr.press/v102/shaw19a.html>.
- R. Shaw, C. H. Sudre, S. Ourselin, and M. J. Cardoso. A Heteroscedastic Uncertainty Model for Decoupling Sources of MRI Image Quality. *arXiv:2001.11927 [cs, eess]*, Jan. 2020. URL <http://arxiv.org/abs/2001.11927>. arXiv: 2001.11927 version: 1.
- C. H. Sudre, M. J. Cardoso, and S. Ourselin. Longitudinal segmentation of age-related white matter hyperintensities. *Medical Image Analysis*, 38:50–64, May 2017. ISSN 1361-8415. doi: 10.1016/j.media.2017.02.007. URL <http://www.sciencedirect.com/science/article/pii/S1361841517300257>.
- S. van der Walt, S. C. Colbert, and G. Varoquaux. The NumPy array: a structure for efficient numerical computation. *Computing in Science & Engineering*, 13(2):22–30, Mar. 2011. ISSN 1521-9615. doi: 10.1109/MCSE.2011.37. URL <http://arxiv.org/abs/1102.1523>. arXiv: 1102.1523.
- K. Van Leemput, F. Maes, D. Vandermeulen, and P. Suetens. Automated model-based tissue classification of MR images of the brain. *IEEE transactions on medical imaging*, 18(10):897–908, Oct. 1999. ISSN 0278-0062. doi: 10.1109/42.811270.

- P. Virtanen, R. Gommers, T. E. Oliphant, M. Haberland, T. Reddy, D. Cournapeau, E. Burovski, P. Peterson, W. Weckesser, J. Bright, S. J. van der Walt, M. Brett, J. Wilson, K. J. Millman, N. Mayorov, A. R. J. Nelson, E. Jones, R. Kern, E. Larson, C. J. Carey, Í. Polat, Y. Feng, E. W. Moore, J. VanderPlas, D. Laxalde, J. Perktold, R. Cimrman, I. Henriksen, E. A. Quintero, C. R. Harris, A. M. Archibald, A. H. Ribeiro, F. Pedregosa, and P. van Mulbregt. SciPy 1.0: fundamental algorithms for scientific computing in Python. *Nature Methods*, pages 1–12, Feb. 2020. ISSN 1548-7105. doi: 10.1038/s41592-019-0686-2. URL <https://www.nature.com/articles/s41592-019-0686-2>.
- wiredfool, A. Clark, Hugo, A. Murray, A. Karpinsky, C. Gohlke, B. Crowell, D. Schmidt, A. Houghton, S. Johnson, S. Mani, J. Ware, D. Caro, S. Kossouho, E. W. Brown, A. Lee, M. Korobov, M. Górný, E. S. Santana, N. Pieuchot, O. Tonnhofer, M. Brown, B. Pierre, J. C. Abela, L. J. Solberg, F. Reyes, A. Buzanov, Y. Yu, eliempje, and F. Tolf. Pillow: 3.1.0, Jan. 2016. URL <https://zenodo.org/record/44297#.X1x04pP7S8o>.
- Y. Yang, L.-F. Yan, X. Zhang, Y. Han, H.-Y. Nan, Y.-C. Hu, B. Hu, S.-L. Yan, J. Zhang, D.-L. Cheng, X.-W. Ge, G.-B. Cui, D. Zhao, and W. Wang. Glioma Grading on Conventional MR Images: A Deep Learning Study With Transfer Learning. *Frontiers in Neuroscience*, 12, 2018. ISSN 1662-453X. doi: 10.3389/fnins.2018.00804. URL <https://www.frontiersin.org/articles/10.3389/fnins.2018.00804/full>.
- J. Zhuo and R. P. Gullapalli. MR Artifacts, Safety, and Quality Control. *RadioGraphics*, 26(1): 275–297, Jan. 2006. ISSN 0271-5333. doi: 10.1148/rg.261055134. URL <https://pubs.rsna.org/doi/full/10.1148/rg.261055134>.